FULL PAPER

Hierarchically Ordered Arrays of Noncircular Silicon Nanowires Featured by Holographic Lithography Toward a High-Fidelity Sensing Platform

*Hwan Chul Jeon, Chul-Joon Heo, Su Yeon Lee, and Seung-Man Yang**

A novel, highly uniform and tunable hybrid plasmonic array is created via ion-milling, catalytic wet-etching and electron-beam evaporation, using a holographically featured structure as a milling mask. A simple and low-cost prism holographic lithography (HL) technique is applied to create an unprecedentedly coordinated array of elliptic gold (Au) holes, which act as the silicon (Si) etching catalyst in the reaction solution used to fabricate an elliptic silicon nanowire (SiNW) array; here, the SiNWs are arrayed hierarchically in such a way that three SiNWs are triangularly coordinated, and the triangles are arranged hexagonally. After removing the polymeric mask and metal thin film, the highly anisotropic thick Au film is deposited on the SiNW arrays. This hybrid substrate shows tunable optical properties in the near-infrared (NIR) region from 875 nm to 1030 nm and surface-enhanced Raman scattering (SERS) activities; these characteristics depend on the catalytic wet etching time, which changes the size of the vertical gap between the Au thick films deposited separately on the SiNWs. In addition, lateral interparticle coupling induces highly intensified SERS signals with good homogeneity. Finally, the Au-capped elliptical SiNW arrays can be hierarchically patterned by combining prism HL and conventional photolithography, and the highly enhanced fluorescence intensity associated with both the structural effects and the plasmon resonances is investigated.

1. Introduction

Periodic metal nanostructures—which can sustain the resonances of collective electron oscillations (known as localized surface plasmon resonances (LSPRs)) when interacting with an incident light field[1]–have been used in a wide range of applications, including plasmonic sensors and novel photonic devices based on the unique properties of such nanostructures.[1–6] LSPR properties can be easily controlled by changing the geometry of the metallic nanostructures and local array environments.[2–6] Surface-enhanced Raman scattering (SERS)-based sensing applications based on the use of plasmonic nanostructures are a prominent research area for the detection of numerous chemical and biological molecules.[7] Enhanced Raman signals—which depend strongly on the type, size, roughness, and shape of the metal nanoparticles, the distance between them, and the excitation wavelength—have been derived from the enhancement of electromagnetic (EM) fields, where the enhancement was the result of the plasmonic resonance excitations.[6,8–15] Various studies have sought to develop suitable SERS substrates with high sensitivity and uniformity. Recently, several research groups demonstrated hybrid SERS substrates in an attempt to exploit the additional enhancement effects; these substrates contained a supporting chemical enhancement between the semiconductors (such as ZnO, TiO_2, CuO and Si) and noble metals, and showed excellent SERS performance.[16–20] However, in spite of the recent advances in the design and fabrication of nanophotonic hybrid structures, a cost-effective, simple, and versatile strategy for the fabrication of uniform and tunable structures over large areas has not yet been achieved with the suitable coordination required for sensing applications. The need for such a method provided the primary motivation for the present study.

Herein, we report a simple and cost-effective method for the fabrication of novel uniform hybrid plasmonic nanostructure arrays, generating lateral and vertical interparticle couplings over a large area via the use of a holographically featured porous structure as a milling mask. Recently, Caldwell et al. fabricated novel SERS substrates using sophisticated electron-beam lithography,[19] which needs a time-consuming serial fabrication procedure for nanostructures over a large-area with demanding precisions. Compared with electron-beam lithography, holographic lithography (HL) is a simple and rapid production technique for one-, two-, and three-dimensional, defect-free periodic structures over large areas using optical interference among coherent light beams.[21–23] However, such conventional multi-beam HL techniques have some disadvantages, including the need for precise beam alignment procedures using a number

H. C. Jeon, Dr. C.-J. Heo, Dr. S. Y. Lee,
Prof. S.-M. Yang
National Creative Research Initiative Center
for Integrated Optofluidic Systems
Department of Chemical and Biomolecular Engineering
Korea Advanced Institute of Science and Technology
335 Gwahangno, Yuseong-gu, Daejeon, 305-701, Korea
E-mail: smyang@kaist.ac.kr

DOI: 10.1002/adfm.201200921

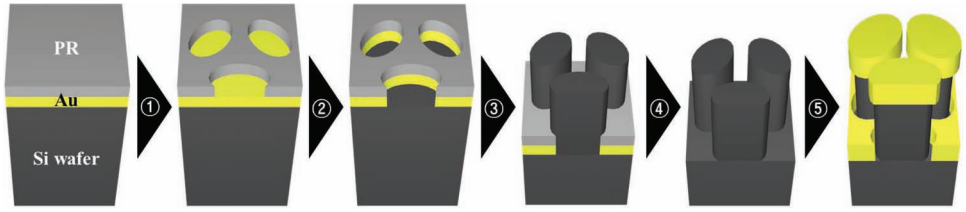

Scheme 1. Schematic of the fabrication of hexagonally ordered, triangularly coordinated three Au-capped elliptical SiNW arrays, using holographic lithographically featured structures. 1) Prism holographic lithography and reactive ion etching to fabricate the polymeric mask on the Au pre-coated Si wafer. 2) Ar ion milling to remove the Au thin film from the vacant spaces. 3) Anisotropic catalytic wet-etching to fabricate triangularly coordinated three elliptical SiNW arrays. 4) Reactive ion etching and Au etching to remove polymeric mask and Au thin film, respectively. 5) Deposition of the Au thick film *via* electron-beam evaporation.

of optical components, and reconfiguration. To overcome such limitations, researchers have recently introduced novel prisms to create multiple beams from a single laser beam, using refraction or total internal reflection.[24,25] HL-featured periodic porous structures have been widely used in templates for the infiltration of polymers or metals,[26–29] the growing of patterned polymer films,[30] and biofunctionalization,[31] as well as in photonic applications.[21–25]

As depicted schematically in **Scheme 1**, the fabrication process consisted of six steps. First, an SU-8 photoresist (PR) was spin-coated on an Si(100) wafer, which had a pre-coated gold (Au) thin film. The thickness of the PR used to fabricate the two-layer face-centered cubic (FCC) structures could be controlled by varying the epoxy-based PR resin concentration, and the spin speed.[6] After soft baking to evaporate the solvent from the polymeric film, HL was carried out to fabricate the double layered FCC structures, using a specially designed prism.[6] The expanded laser beam was passed through a single top-cut prism, thereby splitting one beam into four beams with wave vectors $k_i = 2\pi/\lambda$ ($\cos\beta_i\sin\alpha$, $\sin\beta_i\sin\alpha$, $\cos\alpha$), as derived from Snell's law for a prism with a cutting angle of 54.7° (because of the refraction from the three side surfaces of the prism). In this equation, λ is the wavelength of the laser, and α and β_i are the polar and azimuthal angles of k_i. Post-exposure baking and development were then performed, to accelerate cross-linking and remove unexposed regions, respectively. The resulting double layered FCC structures—consisting of hexagonal arrays of three elliptical holes—were applied as a milling mask. Using Ar ion milling, the Au thin film could be etched from the vacant spaces, such that the Au thin film pattern remaining under the polymeric mask looked like triply split elliptical hole arrays. To achieve novel arrays of well-aligned silicon nanowires (SiNWs), we used an Au-assisted chemical wet etching process in a solution of deionized water, hydrogen peroxide (H_2O_2), and hydrofluoric acid (HF).[32,33] The patterned Au thin film was used as a catalyst in the etching of the underlying Si in the reaction solution; bare Si regions produced by the previous Au milling process were not etched. The length of the SiNWs could be controlled by varying experimental conditions such as concentration of the solution, and the wet etching time. Subsequently, the polymeric mask and the Au thin film were easily removed from the substrate using reactive-ion etching (RIE) and Au etchant solution, respectively. Uniform hexagonal arrays of triangularly coordinated elliptical SiNWs were thus obtained over a large area. Finally, a further Au thick film was deposited on the elliptical SiNW arrays in a highly anisotropic fashion, using electron-beam evaporation.

The resulting novel arrays of hybrid structures exhibited variable optical properties and SERS activities; these properties depended on the heights of the SINWs, variations in which produced differently sized vertical gaps between the Au particles (on the top of the SiNWs) and the triply split elliptical Au hole films (under the SiNWs). Furthermore, high-intensity SERS signals with large-scale sample homogeneity could be achieved using our novel hybrid structure arrays. These signals derived from the higher level of lateral interparticle coupling among the sets of three adjacent Au particles on top of the SINWs, compared with circular SiNW arrays with the same periodicity. The hierarchically patterned hybrid SiNW arrays with adsorbed rhodamine 6G (R6G)—which were obtained by combining prism HL and conventional photolithography[34,35]–showed highly enhanced fluorescence signals compared with a smooth Au film. Our novel hybrid plasmonic structure arrays therefore hold promise for chemical and biomolecular sensing applications based on LSPR or fluorescence.

2. Results and Discussion

Large-area uniform arrays of two-layer FCC structures were obtained via prism HL (Figure S1a, Supporting Information), and were applied as milling masks for the Si(100) wafer, which had a pre-coated 30 nm Au thin film. However, the resulting polymeric mask was relatively 'messy', compared with HL-featured structures made using transparent glass substrates.[6,34,35] For the HL process, transparent substrates are typically used to reduce the reflectance of the beams.[23] We believe that the "messy" nature of our mask might have resulted from additional interference between the incident laser beams and the laser beams reflected or scattered from the metal thin film; this could have influenced the fabrication of the nanostructures. Hence, before the patterning of the Au thin film via the Ar ion milling process, and after the optical patterning, the messy FCC structure was defined using RIE in oxygen plasma, with the aim of removing the residual cross-linked polymers from the two-layer FCC structures. Well-defined two-layer FCC structures that could be used as a milling mask were then be obtained by stripping off the residual polymer (Figure S1b, Supporting Information). Ar ion milling was performed to selectively remove the Au thin film from the vacant three elliptical holes on the Si

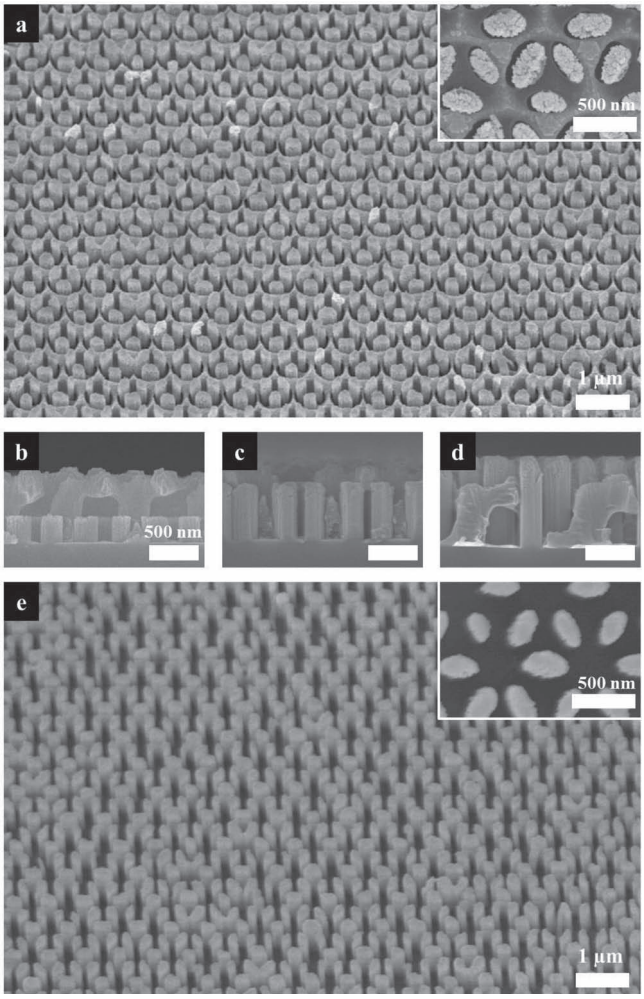

Figure 1. (a) Large-area SEM image of the fabricated hexagonally ordered triangularly coordinated three elliptical SiNW arrays, after 9 min of the catalytic wet etching process. The inset shows a magnified SEM image in the (111) plane. Cross-sectional SEM images of the elliptical SiNW arrays after (b) 3 min, (c) 6 min, and (d) 9 min of the catalytic wet etching process. (e) Large-area SEM image of 9 min etched hexagonally ordered triangularly coordinated three elliptical SiNW arrays, after removing the polymeric mask and the Au thin film. The inset shows a magnified SEM image in the (111) plane.

substrate. To check the patterned shape of the Au thin layer, we preferentially performed O_2 RIE to remove the SU-8 polymeric mask before the standard SiNW fabrication steps were carried out. The resulting Au thin layer was then well etched with a pattern similar to the three-elliptical-hole pattern of the polymeric mask (Figure S1c, Supporting Information).

Novel, large-area SiNW arrays were obtained using Au-assisted chemical wet etching in a solution of 0.44 M H_2O_2 and 4.6 M HF.[32,33] **Figure 1**a shows a tilted-view (ca. 25°) scanning electron microscopy (SEM) image of large-area uniform novel arrays of vertically aligned elliptical SiNWs, after 9 min of catalytic wet etching embedded in a polymeric mask. From the SEM image, we confirmed that three-elliptical SiNWs with triangular coordination were well-ordered in a hexagonal pattern with 710 nm periodicity, over a large area. The inset of Figure 1a shows a magnified image of the resulting SiNW array, in the (111) plane; from this image, the average values for the minor axis (a) and major axis (b) of each elliptical SiNW were measured as a = 173 nm and b = 355 nm, respectively. The length of the nanowires could be easily changed by varying the sample immersion times from 3 min to 9 min. Figures 1b–d show cross-sectional images of elliptical SiNWs with various etched heights, after immersion in the etching solution for 3 min, 6 min, and 9 min, respectively. The polymeric mask remained between the resulting highly anisotropically etched SiNW arrays. Using SEM analysis, the average lengths in the SiNW samples prepared using wet etching times of 3 min, 6 min, and 9 min were found to be 278 nm, 606 nm, and 905 nm, respectively. There was a good correlation between the length of the SiNWs and the duration of the chemical etching, with an estimated etch rate of ~100 nm per minute. After the sample etching process, the removal steps were followed (Figure S2, Supporting Information). The polymeric mask remaining between the well-ordered SiNWs could be easily removed using RIE in oxygen plasma, with a relatively long etching time; this is the method typically used for etching polymers. The polymeric mask was then almost cleanly etched, but the fabricated SiNWs were not affected; a small amount of residual SU-8 polymer remained on the Au thin film. (Figure S2c, Supporting Information). Wet etching was then performed to remove the Au thin film from the Si substrate; this was achieved via immersion for 3 min in an Au etchant solution (Figure S2d, Supporting Information). Only the well-ordered hexagonal arrays of triangularly coordinated three elliptical SINWs remained after the removal process. Figure 1d shows a tilted-view (ca. 25°) SEM image of the large-area, uniformly arranged novel arrays of triangularly coordinated three-elliptical SiNWs, after 9 min wet etching time, and the removal steps. Values of a = 168 nm and b = 348 nm were found, with a periodicity of 710 nm; these values matched well with those for the SiNWs before the removal steps.

Compared with other lithography techniques, the main advantage of HL for the fabrication of 3D structures is that geometric features can be easily controlled by changing the laser exposure time.[6,34,35] In our study, the elliptical hole sizes in the two-layer FCC structures (which determine the aspect ratio of the resulting SiNWs) could be adjusted in this manner (see Figure S3, Supporting Information). As a function of laser dose (increasing from 0.19 sec to 0.21 sec), the hole size in the FCC structures decreased from a = 173 nm and b = 355 nm, to a = 133 nm and b = 251 nm; this resulted in a higher aspect ratio for the same experimental conditions, with only the laser exposure time being varied. Here, the lengths of the nanowires showed similar values at the same etch duration without dependence on the wire diameter. In other words, in the catalytic wet etching process, the length of the etched SiNWs was basically a function of the wet etching time, regardless of other parameters such as diameter or shape of the nanowires; this constituted an advantage compared with other Si etching processes such as vapor-liquid-vapor (VLS) or deep RIE,[36,37] in that the aspect ratio could be easily tuned, simply via careful control over the pore size of the SU-8 polymeric mask.

The 150 nm Au thick film was deposited in a highly anisotropic fashion on the arrays of elliptical SiNWs, using electron-beam

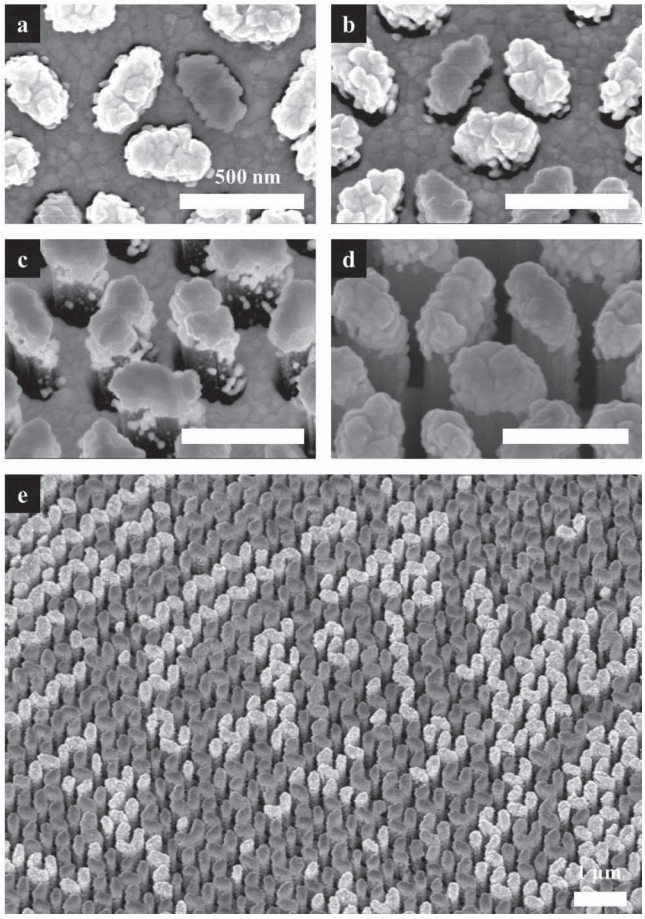

Figure 2. (a) SEM image of the 3 min-etched hexagonally ordered triangularly coordinated three Au-capped elliptical SiNW arrays in the (111) plane. 25° tilted SEM images of the three Au-capped elliptical SiNW arrays after (b) 3 min, (c) 6 min, and (d) 9 min of the catalytic wet etching process. (e) Large-area 25° tilted SEM image of the 9 min-etched hexagonally ordered arrays of triangularly coordinated three Au-capped elliptical SiNWs.

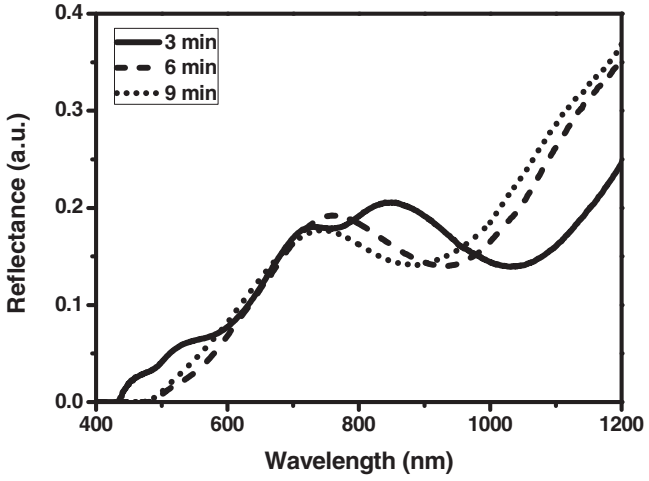

Figure 3. Reflectance spectra measured from hexagonally ordered triangularly coordinated three Au-capped elliptical SiNW arrays with different catalytic wet etching times.

evaporation. The Au film was then separately deposited on top of the elliptical SiNWs, and on the bottom of the SiNWs; this resulted in the two films being isolated from each other, with a vertical gap between them. **Figure 2**a–d show SEM images of Au-capped elliptical SINW arrays obtained using catalytic wet etching times of 3, 6, and 9 min, respectively, while the thickness of the deposited Au film was held constant. The Au particles capping each elliptical SiNWs showed average values of $a = 188$ nm and $b = 367$ nm, for all etching conditions. The increased values for the Au particles capping the SiNWs resulted from the additional, laterally spread deposition of Au film on top of the SiNWs (see Figure S4a,b, Supporting Information). The increasing values for a and b resulted in decreases in the lateral distance between the adjacent three-elliptical SiNWs, from 110 nm to 65 nm. Changes in the height of the SiNWs, which were generated by changing the sample immersion times from 3 min to 9 min, produced different vertical distances between the isolated elliptical Au particles on top of the SiNWs, and the triply split elliptical Au hole arrays under the SiNWs. As the catalytic wet etching time was increased from 3 min to 9 min in 3 min increments, the vertical gap distances increased from 54 nm to 373 nm, and 669 nm (Figure S4c, Supporting Information). There was also a correlation between the vertical distance for the Au-capped SiNWs and the chemical wet etching times, similar to the correlation shown for the height of the etched SiNWs. The geometric features of height and gap of the SiNWs are schematically defined in Figure S4c of Supporting Information. Figure 2e shows a 25° tilted-view SEM image of the vertically aligned Au-capped elliptical SiNW arrays after 9 min of the catalytic wet etching process; the array showed large-area uniformity, and 710 nm periodicity.

The hybrid elliptical SiNW arrays with controllable heights exhibited tunable optical properties. The reflectance spectra of the Au-capped elliptical SiNW arrays are shown in **Figure 3**; these were investigated using a home-built visible-to-near-infrared spectroscopy apparatus, under white light illumination, with normal incidence.[2,6] Reflectance dips were observed in the near-infrared (NIR) regions, and were compared as a function of vertical gap distance. The Au-capped SiNW arrays with 3 min wet etching time exhibited a pronounced reflectance dip at about 1030 nm in the measured reflectance spectrum. As the wet etching time increased—resulting in increases in the size of the vertical gap—the dips in the reflectance spectra were gradually blue-shifted due to changes in the plasmonic resonances and the diffraction responses; these changes were attributed to the variations in the vertical gap in the novel Au-capped elliptical SiNW arrays.[19] The specific spectral positions of the plasmonic resonance strongly depend on the geometric properties of nanostructures, including the size, shape, and arrangement.[2–6] As the vertical gap between the isolated elliptical Au particles on top of the SiNWs and the triply split elliptical Au hole arrays under the SiNWs increased from 54 nm to 373 nm, to 669 nm, the reflection dips associated with the resulting arrays shifted from 1030 nm to 930 nm, to 875 nm. This tunability of the optical properties based on geometric effects holds potential for plasmonic sensing applications.[2–6]

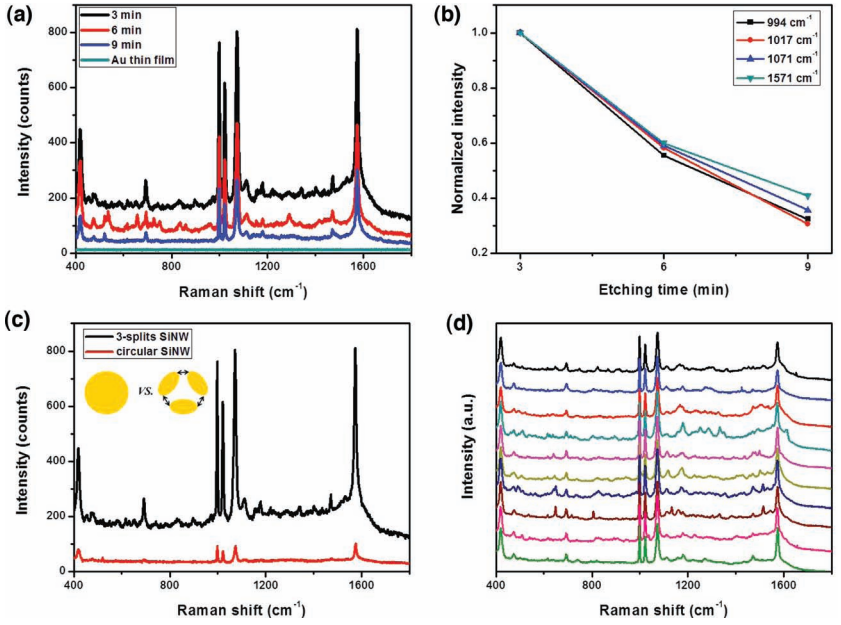

Figure 4. (a) SERS spectra of BT-adsorbed triangularly coordinated three Au-capped elliptical SiNW arrays, under various experimental conditions. (b) Variation of SERS signal intensity of BT-adsorbed three Au-capped elliptical SiNW arrays at 994, 1017, 1071, and 1571 cm^{-1}, as a function of the catalytic wet etching time. (c) Comparison of the measured SERS spectrum for BT adsorption on 3 min-etched triangularly coordinated three Au-capped elliptical SiNW arrays, and one Au-capped circular SiNW arrays. (d) SERS spectra of BT obtained from 10 randomly selected spots on the 3-min etched triangularly coordinated three Au-capped elliptical SiNW arrays. The laser power used on the samples was 75 mW, and data acquisition involved 1.5 sec and 5 sec accumulations for (a, c) and (d), respectively.

The SERS responses of the resulting hybrid plasmonic arrays were observed using 785 nm-wavelength incident light. Benzenethiol (BT) was used as a probe molecule; it was adsorbed on the surfaces of the Au-capped SiNW arrays *via* 12 hour immersion in an ethanolic target-molecular solution. **Figure 4**a shows the SERS activities of the various as-prepared Au-capped SiNW arrays with different vertical gap sizes. As the vertical gap increased in size, the intensity of the SERS signals decreased dramatically. To perform a detailed study of the SERS activity of the resulting arrays, we calculated the normalized intensity of the characteristic BT peaks at 994, 1017, 1071, and 1571 cm^{-1}.[6] Figure 4b shows the variation in SERS intensity for the hybrid plasmonic arrays as a function of the wet etching time, where the intensities were normalized by the intensity for the SiNW arrays etched for 3 min. The data showed that the decrease in intensity for the 3 min-etched samples compared with the 6 min-etched samples was significantly greater than the decrease measured from the 6 min sample to the 9 min sample. The two factors responsible for the enhancement of SERS intensity are a structural resonance wavelength appropriate for the laser excitation wavelength, and the interparticle gap distance.[12–15] As the wet etching time was increased, the blue-shifted structural resonance wavelength was closer to the laser excitation wavelength (see Figure 3), which led to a stronger EM field.[12,13] However, more importantly for this study, the vertical gap distance was dramatically increased under 6 min etching conditions compared with that observed with a 3 min etching time (from 54 nm to 373 nm), which resulted in a weaker plasmon coupling effect;[14,15] hence, the dramatic decrease in the Raman intensity for the 6 min-etched SiNW substrate was a result of the mechanism described here. It is expected that small Au beads deposited onto the side-walls of the SiNWs, and the roughness of the capped elliptical Au particles on tops of the SiNWs can act also as "hot-spots".[10,19] However, our results showed that the feature dimensions of the hierarchical SiNW arrays produce dominant effects, and the vertical and lateral interparticle couplings are the decisive elements for the resulting SERS performance rather than the roughness of deposited Au particles.

Interparticle coupling between the adjacent three-elliptical Au particles on top of the SiNWs strongly increased the magnitude of the local EM fields. The effects of the lateral interparticle gap on the Raman signal enhancement are shown in Figure 4c. The triangularly coordinated three Au-capped elliptical SiNW arrays exhibited a ten-fold increase in Raman intensity over the one Au-capped circular SiNW arrays with same periodicity and wet etching time, which could be fabricated using a single layered FCC structure (Figure S5, Supporting Information).[6] To investigate the effects of vertical gap distance, we also compared the SERS intensity of BT-adsorbed three Au-capped elliptical SiNW arrays with that of analyte-adsorbed triply split elliptical Au hole arrays with 150 nm thickness, which were fabricated *via* an ion-milling process (Figure S6, Supporting Information). More highly intensified Raman signals were obtained from the three Au-capped elliptical SiNW arrays under a 3 min wet etching condition than from the triply split elliptical Au hole arrays. Importantly, the large-scale sample homogeneity of the as-prepared Au-capped elliptical SiNW arrays was also tested, as illustrated in Figure 4d. All of the BT SERS spectra—which were obtained from 10 randomly selected points on the same sample (a 3 min-etched sample)—displayed very similar intensities for the characteristic BT peaks; a 6.9% standard deviation was measured for the peak height at 1017 cm^{-1}, which was in stark value contrast to the previous roughened SERS substrate. These results showed that the primary advantage of prism HL—namely its ability to perform rapid one-spot fabrication of nanostructures over large areas, with high reproducibility[21–23]—was of great use in fabricating the hybrid plasmonic structure arrays.

In addition, hierarchically-patterned Au-capped elliptical SiNW arrays could be obtained by employing an additional UV photomask exposure step to the proposed method.[34,35] **Figure 5**a shows micro-patterned 25 μm hole arrays containing internal two-layer FCC structures, which were fabricated by combining prism HL with conventional photolithography; these functioned as a milling mask for sculpting the underlying Au thin film. The hierarchically-patterned Au-capped elliptical SiNW arrays were prepared following the same fabrication steps as

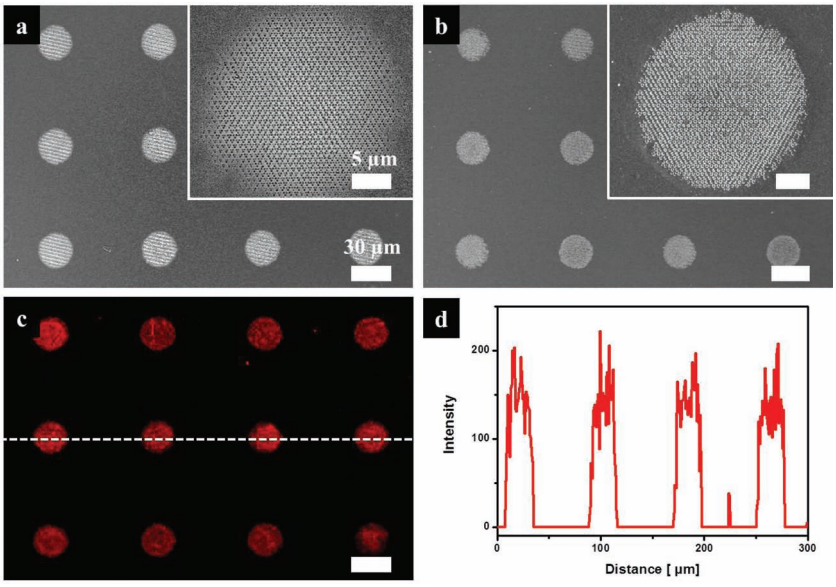

Figure 5. (a) SEM image of hierarchically-patterned polymeric mask, fabricated using holographic lithography and photolithography. Inset shows magnified SEM image. (b) SEM image of hierarchically patterned 6 min-etched Au-capped elliptical SiNW arrays. Inset shows a magnified view of the SEM image. (c) R6G fluorescent intensity from the hierarchically patterned arrays of 6 min-etched Au-capped elliptical SiNWs, and from a flat Au film. (d) The intensity profile from the 6 min-etched three Au-capped elliptical SiNW arrays (where the R6G concentration was 10 μM).

described previously, with a 6 min wet etching duration (see Figure 5b). The inset in Figure 5b shows that the edge of the resulting pattern was irregularly patterned compared with the center, but the internal structures were generally well patterned, with good uniformity. We demonstrated the fluorescence-based sensing capability of the Au-capped elliptical SiNW arrays using the as-prepared sample. The sample was incubated in a 10 μM R6G solution for 30 min, and was then washed with deionized (DI) water, and dried with nitrogen gas. Figure 5c shows that the hierarchically patterned hybrid structures were clearly visible in the images, in contrast with the smooth Au film. The intensity profile (Figure 5d), which was taken by scanning along the horizontal white dotted line in Figure 5c, indicated that the hierarchically patterned region with the Au-capped elliptical SiNW arrays (red-color region) gave a significantly stronger fluorescence signal than the flat Au surface (black-color region) during 30 min under laser irradiation (see Figure S7, Supporting Information). The decrease of fluorescence intensity was caused by photo-degradation of the adsorbed dye molecules under prolonged laser irradiation. The increase in the fluorescence signal from the hybrid plasmonic structures—in comparison with the Au film—was attributed to a combination of 1) the large surface area effect of the hybrid structures causing an increased adsorption capacity for target molecules, and 2) surface-enhanced fluorescence based on the plasmonic extinction of the Au-capped elliptical SiNW arrays.[10,38] These results showed that the hybrid structures have the potential to be applied in SERS- or fluorescence-based chemical and biomolecular sensing applications, when incorporated in microfluidic channels.

3. Conclusions

In summary, novel, large-area uniform arrays of hybrid plasmonic structures were fabricated using prism HL, ion milling, a catalytic wet etching process, and electron-beam evaporation. The resulting hexagonal arrays of triangularly coordinated three Au-capped elliptical SiNWs exhibited tunable plasmonic resonances in the NIR region, and variable SERS activities depending on the changes in the vertical distance—between the Au particles on top of the SiNWs, and the triply split elliptical Au hole films under the SiNWs—that resulted from changes in the sample immersion time. Highly intensified SERS signals with large-scale sample homogeneity were further demonstrated in our novel hybrid structure arrays. These properties, which are superior to those of circular SiNW arrays with same periodicity, can be attributed to the lateral interparticle coupling between adjacent three elliptical Au particles on top of the SINWs. Furthermore, highly enhanced R6G fluorescence signals (compared with a smooth Au film) were achieved using the hierarchically patterned hybrid plasmonic arrays, by combining prism HL and conventional photolithography. Therefore, our novel Au-capped elliptical SiNW arrays—which can generate plasmonic resonances derived from lateral and vertical coupling, and can be easily integrated into microfluidic chips—have the potential to be useful for LSPR- or fluorescence-based chemical and biomolecular sensing applications.

4. Experimental Section

Fabrication of Porous Polymeric Milling Mask: A Si(100) wafer (p-type, resistivity of 1 to 30 Ω-cm) with 30 nm of Au pre-coated on the surface was prepared. SU-8 PR with a resin (EPON SU-8, Miller-Stephenson Chemical)/solvent (γ-butyrolactone (GBL), Sigma-Aldrich) ratio of 4:6 (with photo-initiator (triarylsulfonium hexafluorophosphate salts, Aldrich) 1 wt% to resin) was spun onto the substrate with a spinning speed of 3000 rpm, and a duration of 30 s. After soft-baking on a hotplate at 95 °C for 15 min, an expanded laser beam (He-Cd laser, CW, 325 nm, 50 mW, Kimmon, 1 cm beam diameter) was passed through a single top-cut prism, for an exposure time of 0.19 sec. A detailed description of the optical setup used and the specially designed prism can be found in previous reports.[6,34,35] Post-exposure baking was performed at 55 °C, for 20 min. Finally, unexposed regions were removed using propylene glycol methyl ether acetate (PGMEA, Aldrich), and rinsing was then performed with 2-propanol. The messy SU-8 polymeric structures were then etched using 13.56 MHz RF RIE equipment (Vacuum Science) for confinement. O_2 gas was introduced into the chamber at a flow rate of 100 sccm, and the base pressure was kept at 0.12 Torr, while the RF power was maintained at 100 W for 110 sec in each experiment.

Fabrication of Au-capped Elliptical SiNW Arrays: Ar ion milling (10 sccm, about 2 min) with 400 W DC bias was performed to selectively remove the deposited Au thin film from the vacant spaces on the Si wafer. Triply split Au hole arrays then remained under the polymeric mask. The chemical catalytic wet etching was carried out in a solution consisting of 0.44 M H_2O_2 and 4.6 M HF, for durations of 3 min to

9 min, depending on the length of the nanowires required.[32,33] After the wet etching process, the samples were rinsed in DI water, and dried. The polymeric masks and Au thin film could be removed from the Si substrate *via* etching processes using O_2 RIE (for 8 min, using the same experimental conditions described above), and an Au etchant solution (Gold etch-Type TFA, Transene Comp.) treatment (for 3 min). Finally, the highly anisotropic deposition of a 150 nm-thick Au film was performed on the elliptical SiNW arrays, using an electron-beam evaporator. The resulting Au-capped elliptical SiNW arrays exhibited LSPR, and large-scale sample homogeneity. To evaluate the SERS activities of the samples, they were immersed in ethanolic solutions of 1 mM BT (as an analyte), for 12 hours. The resulting hybrid SERS substrates were then washed with ethanol several times.

Fabrication of Hierarchically Patterned Au-capped Elliptical SiNW Arrays: The hierarchically patterned elliptical SiNW arrays were fabricated by combining prism HL and conventional photolithography.[34,35] After soft-bakingthe PR on the 30 nm Au pre-coated Si wafer, the polymeric films were exposed to 365 nm UV light, which was delivered from a Hg lamp for 80 sec through a photomask containing circular dot arrays with a diameter of 25 μm. Next, a 325 nm laser beam was then shone through a single top-cut prism onto the polymeric films. It is important to note that the SU-8 PR was sensitive to both the 325 nm He-Cd laser source and the 365 nm Hg lamp source. Post-exposure baking, and the development process were then performed. After following the same steps to fabricate arrays of Au-capped elliptical SiNWs, we obtained the hierarchically patterned Au-capped elliptical SiNW arrays. The resulting sample was incubated with 10 μM R6G solution for 30 min, to adsorb molecules to allow the measurement of the fluorescent signal. Finally, the immersed sample was washed with DI water several times, and dried with nitrogen gas.

Characterization: The morphologies of the surface and cross-section of the samples were investigated using a field emission scanning electron microscope (Hitachi S-4800). The optical properties of the resulting samples were analyzed using a home-made visible-to-near-infrared spectroscopy setup for the range of 400–1200 nm with a tungsten-halogen lamp (which produces weak power intensity under ~500 nm). The Raman spectra were measured using a high-resolution dispersive Raman microscope (Horiba JobinYvon, LabRAM HR UV/Vis/NIR), in which a 785 nm laser with a power of 75 mW was focused on the sample surface, which has a diameter of 1 μm. The R6G fluorescence image was obtained using a Zeiss LSM510 laser scanning confocal microscope (Carl Zeiss Inc.), using a 543 nm He-Ne laser.

Supporting Information

Supporting Information is available from the Wiley Online Library or from the author.

Acknowledgements

This work has been supported by a grant from the Creative Research Initiative Program of the Ministry of Education, Science and Technology for "Complementary Hybridization of Optical and Fluidic Devices for Integrated Optofluidic Systems". The authors also appreciated partial support from the Brain Korea 21 Program.

Received: April 1, 2012
Revised: May 11, 2012
Published online: June 18, 2012

[1] W. A. Murray, W. L. Barnes, *Adv. Mater.* **2007**, *19*, 3771.
[2] C. J. Heo, S. H. Kim, S. G. Jang, S. Y. Lee, S. M. Yang, *Adv. Mater.* **2009**, *21*, 1726.
[3] M. Hentschel, M. Saliba, R. Vogelgesang, H. Giessen, A. P. Alivisatos, N. Liu, *Nano Lett.* **2010**, *10*, 2721.
[4] S. Y. Lee, S.-H. Kim, S. G. Jang, C. J. Heo, J. W. Shim, S. M. Yang, *Anal. Chem.* **2011**, *83*, 9174.
[5] A. W. Clark, J. M. Cooper, *Adv. Mater.* **2010**, *22*, 4025.
[6] H. C. Jeon, C. J. Heo, S. Y. Lee, S. G. Park, S. M. Yang, *J. Mater. Chem.* **2012**, *22*, 4603.
[7] K. C. Bantz, A. F. Meyer, N. J. Wittenberg, H. Im, O. Kurtulus, S. H. Lee, N. C. Lindquist, S. H. Oh, C. L. Haynes, *Phys. Chem. Chem. Phys.* **2011**, *13*, 11551.
[8] N. A. Hatab, C. H. Hsueh, A. L. Gaddis, S. T. Retterer, J. H. Li, G. Eres, Z. Zhang, B. Gu, *Nano Lett.* **2010**, *10*, 4952.
[9] D. Choi, Y. Choi, S. Hong, T. Kang, L. P. Lee, *Small* **2010**, *6*, 1741.
[10] L. Y. Wu, B. M. Ross, S. Hong, L. P. Lee, *Small* **2010**, *6*, 503.
[11] S. K. Yang, W. P. Cai, L. C. Kong, Y. Lei, *Adv. Funct. Mater.* **2010**, *20*, 2527.
[12] Y. Yokota, K. Ueno, H. Misawa, *Small* **2011**, *7*, 252.
[13] W. Lee, S. Y. Lee, R. M. Briber, O. Rabin, *Adv. Funct. Mater.* **2011**, *21*, 3424.
[14] L. Gunnarsson, E. J. Bjerneld, H. Xu, S. Petronis, B. Kasemo, M. Kall, *Appl. Phys. Lett.* **2001**, *78*, 802.
[15] J. Ye, M. Shioi, K. Lodewijks, L. Lagae, T. Kawamura, P. van Dorpe, *Appl. Phys. Lett.* **2010**, *97*, 163106.
[16] H. Tang, G. Meng, Q. Huang, Z. Zhang, Z. Huang, C. Zhu, *Adv. Funct. Mater.* **2012**, *22*, 218.
[17] A. Musumeci, D. Gosztola, T. Schiller, N. M. Dimitrijevic, V. Mujica, D. Martin, T. Rajh, *J. Am. Chem. Soc.* **2009**, *131*, 6040.
[18] A. Kudelski, W. Grochala, M. Janik-Czachor, J. Bukowska, A. Szummer, M. Dolata, *J. Raman Spectrosc.* **1998**, *29*, 431.
[19] J. D. Caldwell, O. Glembocki, F. J. Bezares, N. D. Bassim, R. W. Rendell, M. Feygelson, M. Ukaegbu, R. Kasica, L. Shirey, C. Hosten, *ACS Nano* **2011**, *5*, 4046.
[20] Z. Huang, G. Meng, Q. Huang, Y. Yang, C. Zhu, C. Tang, *Adv. Mater.* **2010**, *22*, 4136.
[21] M. Campbell, D. N. Sharp, M. T. Harrison, R. G. Denning, A. J. Turberfield, *Nature* **2000**, *404*, 53.
[22] J. H. Moon, S. Yang, *Chem. Rev.* **2010**, *110*, 547.
[23] J. H. Jang, C. K. Ullal, M. Maldovan, T. Gorishnyy, S. Kooi, C. Y. Koh, E. L. Thomas, *Adv. Funct. Mater.* **2007**, *17*, 3027.
[24] L. J. Wu, Y. C. Zhong, C. T. Chan, K. S. Wong, G. P. Wang, *Appl. Phys. Lett.* **2005**, *86*, 241102.
[25] Y. K. Pang, J. C. W. Lee, C. T. Ho, W. Y. Tam, *Opt. Express* **2006**, *14*, 9113.
[26] S. G. Park, M. Miyake, S. M. Yang, P. V. Braun, *Adv. Mater.* **2011**, *23*, 2749.
[27] M. Miyake, Y. C. Chen, P. V. Braun, P. Wiltzius, *Adv. Mater.* **2009**, *21*, 3012.
[28] Y. Xu, X. Zhu, Y. Dan, J. H. Moon, V. W. Chen, A. T. Johnson, J. W. Perry, S. Yang, *Chem. Mater.* **2008**, *20*, 1816.
[29] J. H. Jang, C. K. Ullal, T. Gorishnyy, V. V. Tsukruk, E. L. Thomas, *Nano Lett.* **2006**, *6*, 740.
[30] H. Fang, D. Yuan, R. Guo, S. Zhang, Ray P. S. Han, S. Das, Z. L. Wang, *ACS Nano* **2011**, *5*, 1476.
[31] S. Singamaneni, E. Kharlampieva, J. H. Jang, M. E. McConney, H. Jiang, T. J. Bunning, E. L. Thomas, V. V. Tsukruk, *Adv. Mater.* **2010**, *22*, 1369.
[32] J. Huang, S. Y. Chiam, H. H. Tan, S. Wang, W. K. Chim, *Chem. Mater.* **2010**, *22*, 4111.
[33] Z. Huang, H. Fang, J. Zhu, *Adv. Mater.* **2007**, *19*, 744.
[34] S. K. Lee, S. G. Park, J. H. Moon, S. M. Yang, *Lab Chip* **2008**, *8*, 388.
[35] S. G. Park, S. K. Lee, J. H. Moon, S. M. Yang, *Lab Chip* **2009**, *9*, 3144.
[36] M. T. Borgstrom, G. Immink, B. Ketelaars, R. Algra, E. P. A. M. Bakkers, *Nat. Nanotechnol.* **2007**, *2*, 541.
[37] K. J. Morton, G. Nieberg, S. Bai, S. Y. Chou, *Nanotechnology* **2008**, *19*, 345301.
[38] E. Fort, S. Gresillon, *J. Phys. D: Appl. Phys.* **2008**, *41*, 013001.